

Coseismic Fluid-Pressure Response Estimated from Prediction-Error Filtering of Tidal-Band Loading

by Timothy L. Masterlark, Herbert F. Wang, Lung S. Chan, and Che Yongtai

Abstract A methodology combining prediction-error filters (PEFs) and transfer functions was developed to identify the quasi-static fluid-pressure response observed in wells due to coseismic strain. Water levels in confined aquifers respond to long-term and seasonal trends, recharge events, barometric and ocean tide loading, tidal strain, and tectonic strain. Low-frequency features can be neglected from the quasi-static coseismic response estimation. Transfer functions were constructed to deconvolve the fluid-pressure response due to measured barometric loading. Because direct tidal strain and ocean tide loading measurements are rarely available, theoretical tidal loading is often calculated from astronomical data. However, the calculations are subject to many assumptions. Because tidal driving processes are cyclic, PEFs are a natural choice for removing the fluid-pressure response without assuming a theoretical forcing function in the tidal band. The method was applied to hourly fluid pressure data collected over a 3-year period from two wells in the villages of Gaocun and Tayuan, China. Results of this analysis yielded coseismic fluid pressure heads of -1.6×10^{-2} and $+7.6 \times 10^{-2}$ m for the respective wells in response to the Datong–Yanggao earthquake swarm mainshock (M_s 6.1), 18–24 October 1989. Epicentral distances to the wells were about 200 km. The coseismic fluid-pressure response for each well was also predicted from dislocation model strain scaled by material-dependent volumetric strain sensitivity parameters. These parameters were determined from the static confined response to O_1 and M_2 earth-tide strain constituents. The predicted response was -2.9×10^{-3} m for the Gaocun well and $+2.1 \times 10^{-3}$ m for the Tayuan well. Although predicted and observed response phases were consistent, both predictions underestimated observed response amplitudes, as has been true in other reported instances.

Introduction

Many studies suggest wells can be sensitive crustal strain meters under certain conditions. The quantitative study of groundwater fluctuations due to barometric loading and tidal strain yields important information about aquifer poroelastic properties (Bredehoeft 1967; Van der Kamp and Gale, 1983; Roeloffs, 1995) and anomalous behavior attributed to tectonic activity (Igarashi and Wakita, 1991; Chen *et al.*, 1993; Roeloffs and Quilty, 1997).

In previous studies, various filters were devised to remove the fluid-pressure response to barometric loading, tidal strain, and ocean tide loading. Assuming quasi-static confined (undrained) conditions, scaling coefficients were used to remove the fluid-pressure response to barometric loading and tidal strain. Sterling and Smets (1971) and Beavan *et al.* (1991) assumed bandlimited undrained conditions for their analyses. However, residuals from the analysis performed by Beavan *et al.* (1991) contained periodicity in the tidal band. Hackbarth (1982) performed an undrained analysis

that resulted in time-dependent phase lags between earth tide strain and fluid pressure. Roeloffs and Quilty (1997) assumed a univariate frequency-dependent fluid-pressure response to barometric loading and allowed for phase shifts in the response to tidal strain. Igarashi and Wakita (1991) and Kitagawa and Matsumoto (1996) estimated multivariate transfer functions that included both barometric pressure and theoretical earth tide strain in the input signals. The removal of tidal band fluid-pressure response with these methods has been accomplished with moderate success.

All of these methods rely on calculated theoretical earth tide strain and ocean tide loading signals to generate tidal band forcing functions. Natural deviations from the earth tide strain calculation assumptions can introduce unknown error (Igarashi and Wakita, 1991). Another potential problem with these methods arises if the fluid-pressure signal is contaminated with local tectonic strain signals. This local signal contamination may cause significant deconvolution

problems (Wei, 1994). Because the coseismic fluid-pressure response is a singular event, signal reduction with multivariate transform functions produces a smeared version of the true coseismic fluid-pressure response.

The purpose of this study was to introduce a methodology combining univariate transfer functions for barometric effects and prediction-error filters (PEFs) and outlier analysis for tidal effects to obtain coseismic fluid-pressure behavior. The method produced results without theoretical tidal band bias found in prior analyses. The method was applied to two wells in northeastern China to identify potential coseismic water-level changes due to a magnitude M_s 6.1 earthquake. Epicentral distances to the wells were about 200 km. The water-level changes were compared to dislocation model strain predictions scaled by volumetric strain sensitivity coefficients.

Water-Level Data

The study site is located in the Shanxi rift system in the counties of Datong and Yanggao, northeast China. Xu *et al.* (1992) discussed the geology and tectonic structure of the area in detail. From 18 to 24 October 1989, a sequence of earthquakes, referred to as the Datong–Yanggao earthquake swarm, interrupted a 175-year period of regional seismic inactivity. Fluid-pressure and corresponding barometric pressure time series data were collected from two monitoring stations located near the villages of Gaocun (GC) and Tayuan (TY), China. Well locations and epicentral distances are shown in Figure 1. The GC well has an uncased interval in a carbonate aquifer 3402 m deep. The TY well is open in an andesite tuff aquifer at a depth of 362 m. Well logs and local geology suggest both wells are open in confined aquifers. The deep GC well carbonate aquifer is confined by almost

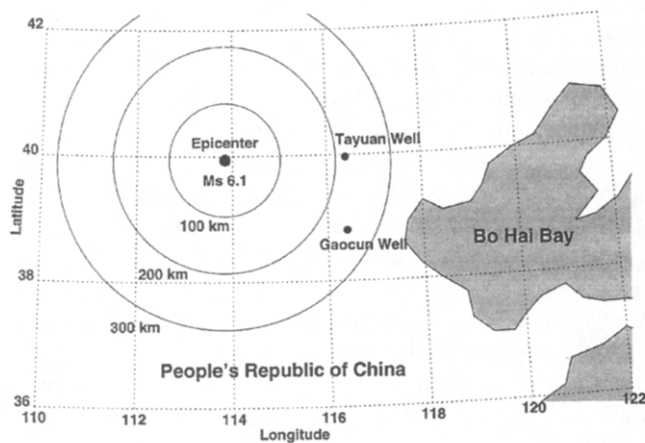


Figure 1. The study site is located in North East China. The mainshock of the Datong–Yanggao earthquake swarm occurred on 19 October 1989. Water-level data were collected from the Gaocun and Tayuan wells from 1988–1990. Epicentral distances to the wells are about 200 km.

2000 m of overlying sand and limestone argillite. The TY well andesite tuff aquifer is capped by a layer of argillite slate 59 m thick. Transfer functions with relatively flat amplitude and phase response introduced later in this article also suggest bandlimited undrained conditions. Well bore diameters are 0.108 and 0.130 m for the GC and TY wells, respectively. The relatively small diameters of these wells minimize transient well bore storage effects under confined conditions (Bredehoeft, 1967; Beavan *et al.*, 1991).

Measurements were taken hourly over a 3-year period from the beginning of 1988 through 1990 (Figs. 2 and 3). Water-level data were recorded with pressure transducers to ± 1.0 mm. Barometric pressure measurements were accurate to ± 0.1 kPa. Precipitation data were also collected to ± 0.1

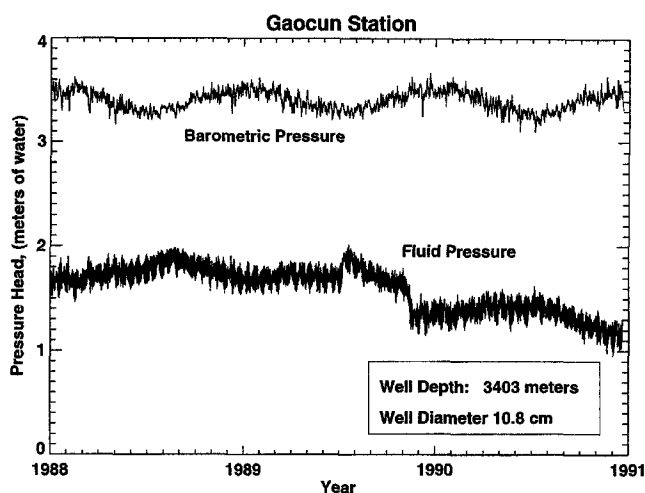


Figure 2. Water levels and barometric pressure data were collected during the period 1988–1990. The data are expressed as pressure head with respect to an arbitrary datum.

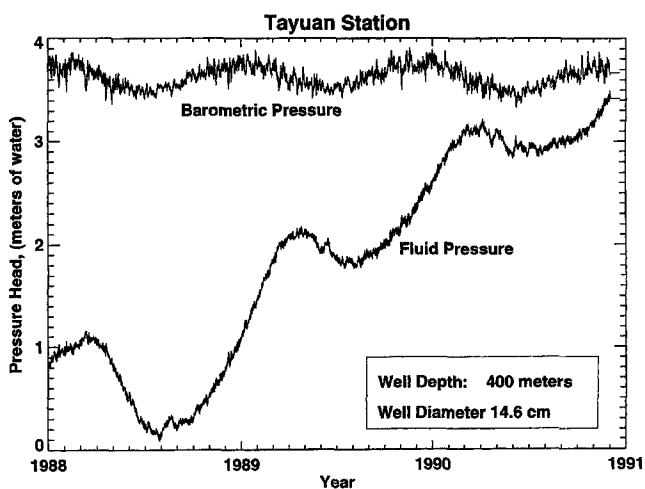


Figure 3. Water levels and barometric pressure data were collected during the period 1988–1990. The data are expressed as pressure head with respect to an arbitrary datum.

mm from the two monitoring stations during the interval 1989–1990. The data included missing intervals, instrument recalibration, and outliers. Gross outliers were noted and replaced with interpolated values. Missing intervals of less than 6 hrs were interpolated. The Chinese State Seismological Bureau completed a study of long-term statistics and characteristics of water-level behavior exhibited in the region (Che and Yu, 1993), but we do not attempt to further discuss low-frequency climatic, transient seasonal, or recharge-related phenomena.

The fluid-pressure time series contains both predictable and unpredictable components. Predictable elements can be separated into three frequency-based categories: (1) low-frequency components that include climatic trends and seasonal periodicity, (2) intermediate-band barometric pressure fluctuations, and (3) high-frequency tidal band forcing. Because the coseismic response is on the order of days, we need not consider low-frequency signals. In this article, fluid pressure (P_f) and barometric pressure (P_b) are expressed as pressure head.

Barometric Loading

Our two-step reduction procedure for the water-level time series begins by removing the barometric-loading component. For undrained conditions, the fluid-pressure response to broadband barometric pressure fluctuations and high-frequency tidal band forcing is well defined. The barometric efficiency is the ratio of the fluid-pressure response in an open well to an applied barometric stress (Jacob, 1940; Wang 1993).

Because barometric loading occurs over a range of frequencies, we assume a more general frequency-dependent fluid-pressure response to account for pressure diffusion and finite-well bore storage (Quilty and Roeloffs, 1991); that is, the convolution of the barometric loading signal ($P_b[t]$) and the system response ($H[t]$) gives the fluid-pressure response $P_f(t)$:

$$P_f(t) = H(t) * P_b(t). \quad (1)$$

The Fourier transform is

$$P_f(\Omega) = H(\Omega)P_b(\Omega). \quad (2)$$

Transfer functions ($\hat{H}[\Omega]$) were constructed to estimate $H(\Omega)$ for the individual wells according to the method described by Quilty and Roeloffs (1991). The term $\hat{H}(\Omega)$ can be determined from the ratio of the barometric loading and fluid-pressure cross spectrum ($P_{bf}[\Omega]$) and the barometric loading autospectrum ($P_{bb}[\Omega]$):

$$\hat{H}(\Omega) = \frac{P_{bf}(\Omega)}{P_{bb}(\Omega)}. \quad (3)$$

It is useful to separate the transfer function into gain and phase components:

$$|\hat{H}(\Omega)| = \frac{|P_{bf}(\Omega)|}{|P_{bb}(\Omega)|} \equiv \text{gain}, \quad (4)$$

$$\angle \hat{H}(\Omega) = \angle P_{bf}(\Omega) - \angle P_{bb}(\Omega) \equiv \text{phase}. \quad (5)$$

Bandlimited undrained conditions prevail if the gain is constant and the phase is 180° over the bandwidth of interest. Because the foregoing conditions are reasonably met in both wells, undrained conditions are approximated for barometric-loading frequencies between 0.02 cpd and the tidal band (Figs. 4 and 5). For these conditions, $\hat{H}(t)$ becomes a scaled delta function (δ), and the convolution is

$$P_f(t) = P_b(t) * (b_e \delta), \quad (6)$$

where b_e is the barometric efficiency:

$$b_e = -\left(\frac{P_f}{P_b}\right). \quad (7)$$

The negative sign accounts for the 180° phase shift. Although the barometric efficiency simplifies to a constant in this analysis, the method allows for frequency-dependent barometric efficiencies.

Tidal Loading

The second signal-reduction step is to determine the fluid-pressure response to tidal band loading. In previous analyses, the earth-tide component of the fluid-pressure signal was removed by subtracting the scaled theoretical tidal strain from the fluid-pressure signal. Precise estimations of

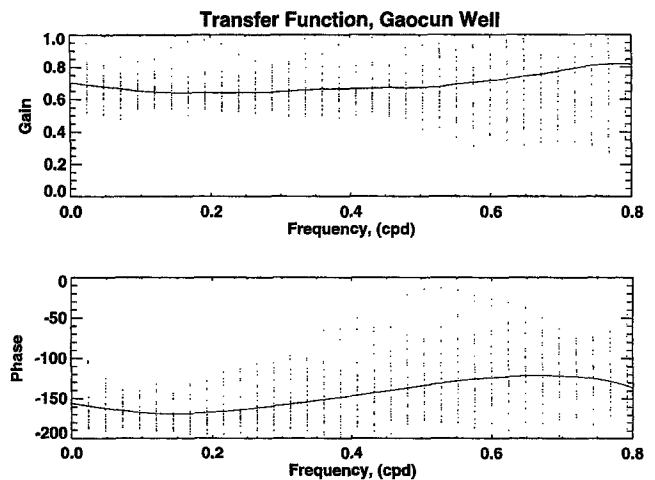


Figure 4. Gaocun well barometric loading transfer function is separated into gain and phase components. The total data set was separated into 34 realizations. Quasi-static barometric efficiency is estimated as 0.7.

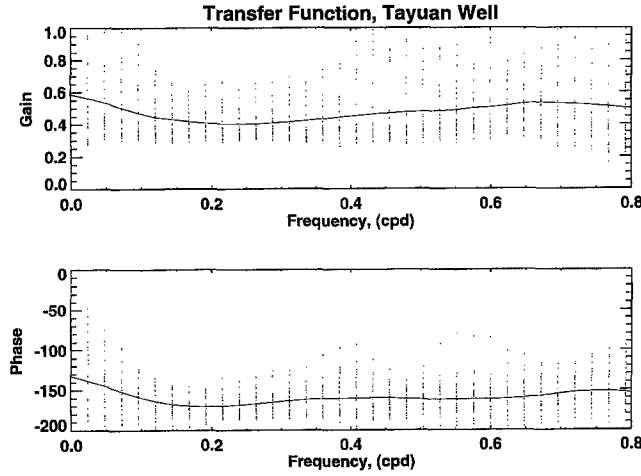


Figure 5. Tayuan well barometric loading transfer function is separated into gain and phase components. The total data set was separated into 26 realizations. Quasi-static barometric efficiency is estimated as 0.5.

theoretical tidal potential (W) may be calculated from astronomical data (e.g., Harrison, 1971). The transformation of theoretical tidal potential to volumetric earth tide strain (ε_{kk}) is

$$\varepsilon_{kk} = \left(\frac{1 - 2\nu}{1 - \nu} \right) \left[(2\bar{h} - 6\bar{l}) \frac{W}{rg} \right]. \quad (8)$$

The relationship assumes a spherical, homogeneous, layered earth model with a free surface and global Love numbers \bar{h} and \bar{l} describing homogeneous stratified density and elastic properties, where ν is Poisson's ratio, r is the Earth's radius, and g is gravitational acceleration (Melchoir, 1983). A volumetric strain sensitivity coefficient (E_s) describes the poroelastic fluid-pressure response to quasi-static volumetric strain (Roeloffs, 1995):

$$E_s = -\frac{P_f}{\varepsilon_{kk}} = -\left(\frac{1}{\rho_f g} \right) \frac{3(1 - 2\nu_u)}{2BG(1 + \nu_u)}, \quad (9)$$

where ν_u is the undrained Poisson's ratio, B is Skempton's coefficient, G is the shear modulus, and ρ_f is the fluid density. Omitting corrections for ocean tide loading can produce errors up to 44%, while tidal strains corrected for ocean tide loading may include 10% error (Beaumont and Berger, 1975).

Prediction-Error Filters

In this article, a PEF technique was developed to estimate the tidal band fluid-pressure response signals. This technique bypasses theoretical tidal strain and ocean tide loading calculation uncertainties and accounts for diurnal thermal barometric loading variations (Roeloffs, 1995). PEFs are a class of Wiener filters developed for and used exten-

sively in reflection seismology for reverberation deconvolution. This technique was combined with outlier analysis methods to identify local coseismic response signals and contamination. The strong deterministic nature of tidal strain and ocean tide loading is ideal for this type of analysis (Robinson and Treitel, 1980; Press *et al.*, 1986; Clay, 1990). PEFs are least-squares autoregressive (AR) models that use a predetermined number of prior consecutive data points to predict future values. The prediction error is the difference between actual and predicted values. Outlier analysis was utilized to remove potential outliers and minimize subsequent reverberation. This procedure was repeated for each sequential data point in the fluid-pressure time series. Since the filter coefficients evolve for each sequential prediction, the method was capable of accounting for signal drift and lunar and solar orbit phase interference. The methods were applied to fluid-pressure time series corrected for barometric loading with transfer functions.

Filter Model Selection

Long-period trends and tidal band phase interference typically found in fluid-pressure time series data indicate nonstationarity in the time series mean and variance. Ideally, seasonal integrated autoregressive moving average (ARIMA) models could be constructed to represent nonstationary seasonal models. However, the number of seasonal terms and period lengths necessary to represent tidal band complexities is too cumbersome for seasonal differencing operations. Alternatively, ARIMA models can be represented by truncated AR representations

$$\tilde{P}_{f(t+k)} = \sum_{i=1}^p \phi_i P_{f(t+k-i)} + \tilde{\varepsilon}_{(t+k)} \quad (10)$$

because we are interested in predicting dominant tidal band-limited periodicity, where \tilde{P}_f is the predicted value, ϕ_i is an AR coefficient, $\tilde{\varepsilon}$ is prediction error, and p is model order. Wei (1994) discussed this type of model in detail.

Reverberation deconvolution in stationary signals requires parameters for filter length (p) and prediction length (k). Because our processes were nonstationary, we limited the prediction length to $k = 1$. Model order selection is somewhat subjective (Clay, 1990). The number of terms chosen for a model was based on three criteria. First, the AR(p) model must contain enough terms ($p \geq 25$) to capture tidal band periodicity. Second, model error is minimized by fitting an AR(p) model such that estimated total model prediction error ($\bar{\sigma}$) is minimized, where n is the number of data points:

$$\bar{\sigma} = \left[\frac{1}{(n-p)} \sum_{t=(p+1)}^n (\tilde{\varepsilon}_t)^2 \right]^{1/2}. \quad (11)$$

Lastly, the principle of parsimony indicates a minimal model order satisfying the first two criterion should be selected for

prediction efficiency and computational stability. Filter lengths of 28 and 32 hr were chosen for the TY and GC wells, respectively (Figs. 6 and 7).

Filtering Procedure

A selected AR(p) model was fitted to the first p data points and used to predict $\tilde{P}_{f(t+1)}$. Prediction error is

$$\tilde{e}_{t+1} = P_{f(t+1)} - \tilde{P}_{f(t+1)}. \quad (12)$$

The prediction error is a combination of noise and outlier contamination. Long-period seasonal correlations were assumed negligible. Outliers can seriously bias parameter estimations and residual error variance. An iterative outlier detection method described by Wei (1994) was used to identify and remove potential innovations (I) at time $= \tau$ based on a predetermined estimated noise threshold (C). A threshold value of $C = 3$ was chosen to allow prediction errors up to three standard deviations.

$$I_{\tau} = \begin{cases} 1 & \text{if } \frac{\tilde{e}_{\tau}}{\bar{\sigma}} \geq C, \\ 0 & \text{if } \frac{\tilde{e}_{\tau}}{\bar{\sigma}} < C. \end{cases} \quad (13)$$

Initial estimates for $\bar{\sigma}$ were 0.005 and 0.003 m based on preliminary filter results for the GC and TY wells, respectively. An innovation takes the form of a spike ($\omega_{A[\tau]}$) or step ($\omega_{I[\tau]}$) outlier.

$$\omega_{A(\tau)} = \begin{cases} \tilde{e}_{\tau} I_{\tau} & \text{if } t = \tau, \\ 0 & \text{if } t \neq \tau, \end{cases} \quad (14)$$

$$\omega_{I(\tau)} = \begin{cases} \tilde{e}_{\tau} I_{\tau} & \text{if } t \geq \tau, \\ 0 & \text{if } t < \tau. \end{cases} \quad (15)$$

If local innovations are not removed, reverberation will contaminate the next p subsequent predictions and potentially overwhelm sought-for coseismic anomalies. After potential outliers are removed, the model then slides one time step ahead, new AR coefficients are calculated, and the next prediction error is determined. This procedure was repeated over the entire fluid-pressure time series to produce separate residual and outlier signals. Addition of the integrated residual signal and the innovation signal produces a filtered fluid-pressure signal (\bar{P}_f) with the barometric loading and tidal band response components removed.

$$\bar{P}_{f(t)} = \omega_{A(t)} + \omega_{I(t)} + \sum_{t=(p+1)}^n (\tilde{e}_t + \tilde{e}_{t-1}). \quad (16)$$

Filtered fluid-pressure signals from both wells are given in Figures 8 and 9. Coseismic fluid-pressure outliers of -0.016 and $+0.076$ m with final residual standard deviation estimates of $\bar{\sigma}_{GC} = 0.0052$ and $\bar{\sigma}_{TY} = 0.0032$ m were determined for the GC and TY wells, respectively. Signal processing parameters and results are summarized in Table 1.

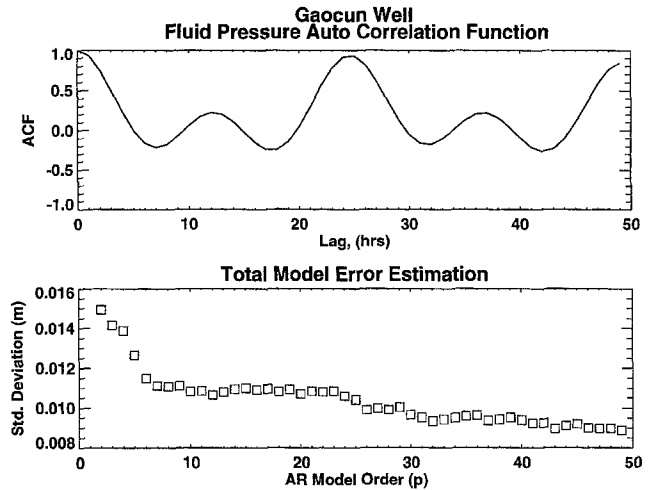


Figure 6. Model order selection criteria. Dominant tidal band peaks at 12 and 25 hr are apparent in the autocorrelation function plot. Model order of $p = 32$ was chosen for the Gaocun well; because this was sufficient to capture tidal band periodicity, a total model error minima occurs at $p = 32$, and additional terms would not significantly improve model performance.

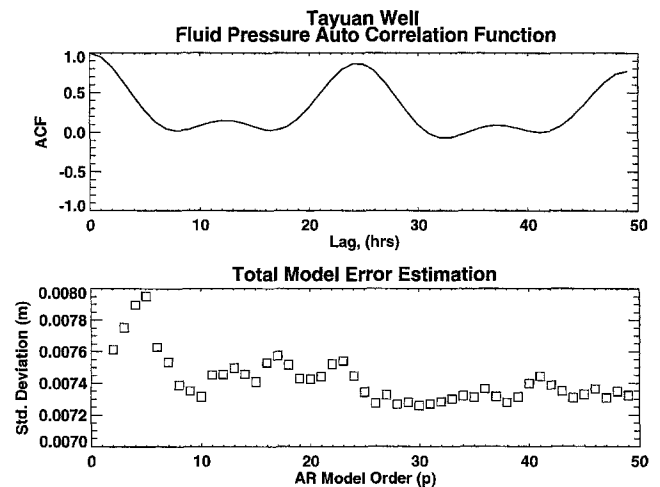


Figure 7. Model order selection criteria. Dominant tidal band peaks at 12 and 25 hr are apparent in the autocorrelation function plot. Model order of $p = 28$ was chosen for the Tayuan well; because this was sufficient to capture tidal band periodicity, a total model error minima occurs at $p = 28$, and additional terms would not significantly improve model performance.

Although the coseismic response for the TY well was obvious, our method allowed us to quantify it as a least-squares estimation. The method was particularly well suited for the GC well data because the response magnitude approached the signal detection resolution limit of $3\bar{\sigma}_{GC}$. Other methods might have smeared the GC coseismic response such that it may have been lost in signal noise.

Dislocation Model

An analytical dislocation model was constructed from Okada's (1992) solution for strain due to a finite dislocation in an elastic half-space. Fault-plane solution data from the Datong-Yanggao earthquake swarm, mainshock M_s 6.1,

were used as input. Fault dimensions were estimated from the aftershock distribution (Xu *et al.*, 1992). The magnitude of the dislocation vector (\bar{u}) was estimated from

$$M_0 = G\bar{u}A, \tag{17}$$

where M_0 is the seismic moment and A is the fault area (Aki and Richards, 1967). Table 2 summarizes the dislocation model parameters. The dislocation was primarily left lateral on a high angle fault. This configuration predicted a strike-slip quadrantal coseismic strain field. Both wells were located in regions undergoing about one nanostrain (Fig. 10).

The volumetric strain sensitivity coefficients were estimated by determining the ratios of fluid-pressure response amplitudes to O_1 and M_2 theoretical earth-tide strain ampli-

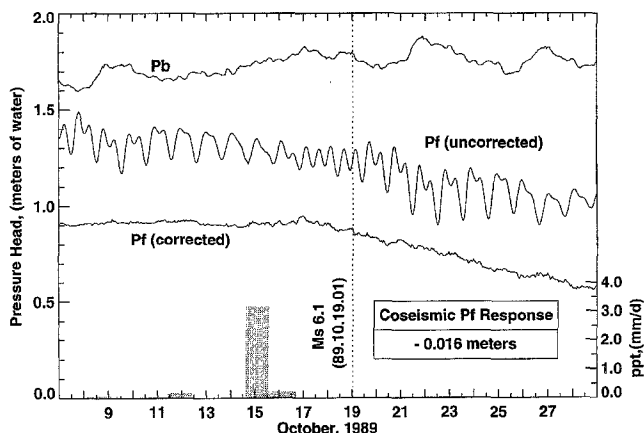


Figure 8. Gaocun well data results. Water-level data were separated into barometric loading and tidal band components. The histogram represents precipitation data. The residual water-level signal, P_f (corrected), shows a coseismic water-level drop, although its magnitude approaches the detection resolution limit.

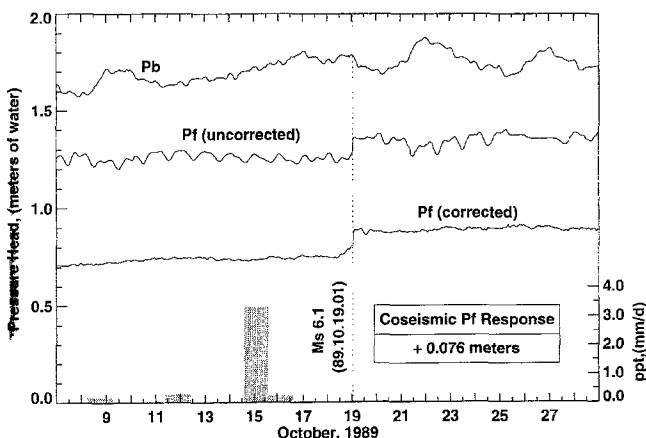


Figure 9. Tayuan well data results. Water-level data were separated into barometric loading and tidal band components. The histogram represents precipitation data. The residual water-level signal, P_f (corrected), shows a coseismic water level increase.

Table 1
Signal Processing Results

Parameter	Gaocun Well	Tayuan Well
\bar{P}_f (m)	-0.016	+0.076
$\bar{\sigma}$ (m)	5.2×10^{-3}	3.2×10^{-3}
p	32	28

Table 2
Dislocation Model Parameters

Parameter	Dislocation Model
G (Pa)	4.0×10^{10}
ν_u	0.33
Focus depth (m)	1.4×10^4
Fault strike	11°
Fault dip	80°
Fault length (m)	1.4×10^4
Fault width (m)	1.4×10^4
M_0 (Nm)	7.0×10^{18}
A (m ²)	1.96×10^8
\bar{u} (m)	0.89

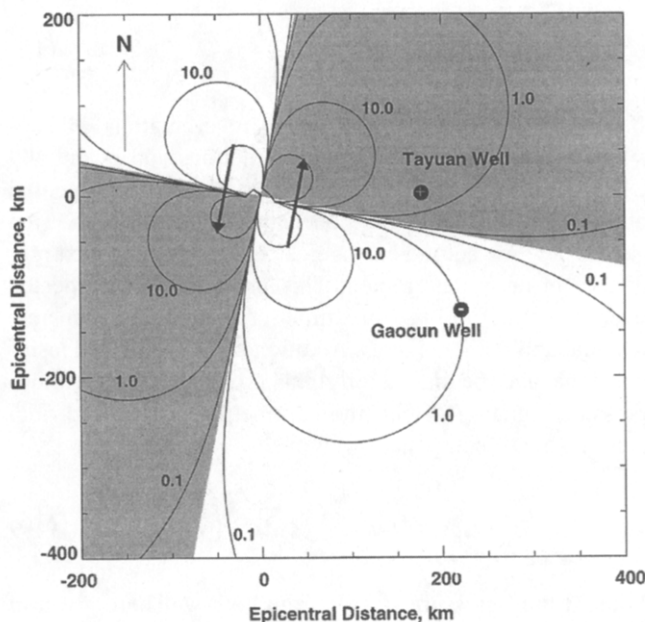


Figure 10. Predicted coseismic strain. Contour plot of volumetric nanostrain resembles a quadrantal pattern. Shaded areas represent compression. Heavy arrows near epicenter express the relative left-lateral displacement.

Table 3
Volumetric Strain Sensitivity

Parameter	Gaocun Well		Tayuan Well	
	O_1	M_2	O_1	M_2
ϵ_{kk} amplitude	3.2×10^{-9}	4.4×10^{-9}	3.9×10^{-9}	4.5×10^{-9}
P_f (m)	0.0096	0.012	0.0032	0.0050
E_s (m^{-1})	-2.9×10^6		-0.97×10^6	

Table 4
Dislocation Model Results

Parameter	Gaocun Well	Tayuan Well
\hat{P}_f (m)	-2.9×10^{-3}	$+2.1 \times 10^{-3}$
ϵ_{kk}	$+1.0 \times 10^{-9}$	-2.2×10^{-9}
E_s (m^{-1})	-2.9×10^6	-0.97×10^6

tudes, assuming static confined conditions (Roeloffs, 1995). The volumetric earth-tide strain was estimated to be the average of the resulting O_1 and M_2 constituent ratios (Igarashi and Wakita, 1991) (Table 3). The two wells are on opposite sides of the nodal plane, and the predicted coseismic response (\hat{P}_f) from each well was consistent in phase. However, the dislocation model predicted amplitudes well below the noise threshold and underestimated the observed coseismic response of both wells. This result was expected for the TY well based on its unusually large far-field observed fluid-pressure response. Table 4 summarizes dislocation model results.

Conclusions

Transfer functions for barometric effects and PEFs combined with outlier analysis techniques for tidal band loading provide powerful tools for fluid-pressure time series data decomposition. The method allows removal of the tidal band fluid-pressure response without specifying theoretical forcing functions. The method provides a quantitative means to estimate coseismic fluid-pressure response signals. Dislocation model and observed response phases were consistent, although the dislocation model predictions underestimated GC and TY observed response amplitudes. Predicted amplitude underestimations for far-field coseismic fluid-pressure behavior were similar to discrepancies reported by Igarashi and Wakita (1991), Che *et al.* (1993), and Roeloffs *et al.* (1995). Deviations from assumed homogeneous isotropic conditions in elastic strain models provide possible explanations for these discrepancies. In addition, the three-dimensional strain sensitivity coefficients contain unknown error due to deviations from the assumptions of that analysis, such as the influence of fractures.

Acknowledgments

This research was funded in part by a Hong Kong RGC grant and a University of Hong Kong CRGC grant. Partial support for H.F.W. provided

by NSF grant EAR96-14558 and USGS NEHRP grant 902899HQGR0016. Funding for T.L.M. was provided by NASA ESS Fellowships ESS/98-0000089 and R-ESS/99-0000015. Travel expenses were provided in part by the Exxon Foundation Field Research Grant 133-S317.

References

- Aki, K., and P. G. Richards (1980). *Quantitative Seismology: Theory and Methods*, Vol. 1., W.H. Freeman and Company, San Francisco, 49.
- Baumont, C., and J. Berger (1975). An analysis of tidal strain observations from the United States of America. I: The laterally homogeneous tide, *Bull. Seism. Soc. Am.* **65**, 1613–1629.
- Beavan, J., K. Evans, S. Mousa, and D. Simpson (1991). Estimating aquifer parameters from analysis of forced fluctuations in well levels: an example from the Nubian formation near Aswan, Egypt, 2. Poroelastic properties, *J. Geophys. Res.* **96**, 12139–12160.
- Bredehoeft, J. D. (1967). Response of well-aquifer systems to Earth tides, *J. Geophys. Res.* **72**, 3075–3087.
- Che Yongtai and Yu Jinzi (1993). Structural activity of Datong-Yanggao earthquake and characteristics of groundwater behavior field, *J. Earthquake Pred. Res.* **2**, 315–328.
- Che Yongtai, Yu Jinzi, and Tang Yi (1993). The earthquake-response theory and earthquake prediction method of groundwater dynamics, *J. Earthquake Pred. Res.* **2**, 571–584.
- Clay, C. S. (1990). *Elementary Exploration Seismology*, Prentice Hall, Englewood Cliffs, New Jersey, 289–294.
- Hackbarth, D. A. (1982). Water level fluctuations due to earth tides at Peshtigo, Wisconsin, *Geosci. Wis.* **6**, 1–10.
- Harrison, J. C. (1971). New computer programs for the calculation of earth tides, in *Report of the Cooperative Institute for Research in Environmental Sciences*, University of Colorado, Boulder.
- Igarashi, G., and H. Wakita (1991). Tidal responses and earthquake-related changes in the water level of deep wells, *J. Geophys. Res.* **96**, 4269–4278.
- Jacob, C. E. (1940). On the flow of water in an elastic Artesian aquifer, *Trans. Am. Geophys. Union* **21**, 574–586.
- Kitagawa, G., and N. Matsumoto (1996). Detection of coseismic changes of underground water level, *J. Am. Stat. Assoc.* **91**, 521–528.
- Melchior, P. (1983). *The Tides of the Planet Earth*, Second Ed. Pergamon, Oxford.
- Okada, Y. (1992). Internal deformation due to shear and tensile faults in a half-space, *Bull. Seism. Soc. Am.* **82**, 1018–1040.
- Press, W. H., B. P. Flannery, S. A. Teukolsky, and W. T. Vetterling (1986). *Numerical Recipes*, Cambridge University Press, Cambridge, 423–428.
- Quilty, E. G., and E. A. Roeloffs (1991). Removal of barometric pressure response from water level data, *J. Geophys. Res.* **96**, 10209–10208.
- Robinson, E. S., and S. Treitel (1980). *Geophysical Signal Analysis*, Prentice Hall Signal Processing Series, Prentice-Hall, Englewood Cliffs, New Jersey, 22–29, 238–294.
- Roeloffs, E. A. (1995). Poroelastic techniques in the study of earthquake-related hydrologic phenomena, *Adv. Geophys.* **37**, 135–195.
- Roeloffs, E. A., and E. G. Quilty (1997). Water level and strain changes preceding and following the August 4, 1985 Kettleman Hills, California, earthquake, *Pageoph* **149**, 21–60.
- Roeloffs, E. A., W. R. Danskin, C. D. Farrar, D. L. Galloway, S. N. Hamlin, E. G. Quilty, H. M. Quinn, D. H. Schaefer, M. L. Sorey, D. E. Woodcock (1995). Hydrologic effects associated with the June 28, 1992 Landers, California, earthquake sequence, *U.S. Geol. Surv. Open-File Rept.* 95-42.
- Sterling, A., and E. Smets (1971). Study of earth tides, earthquakes and terrestrial spectroscopy by analysis of the level fluctuations in a borehole at Heibaart (Belgium), *Geophys. J. R. Astr. Soc.* **23**, 225–242.
- Van der Kamp, G., and J. E. Gale (1983). Theory of earth tide and barometric effects in porous formations with compressible grains, *Water Resource. Res.* **19**, 538–544.

Wang, H. F. (1993). Quasi-static poroelastic parameters in rock and their geophysical applications, *Pageoph* **141**, 269–286.

Wei, W. W. S. (1994). *Time Series Analysis*, Addison-Wesley, New York, 42–46 86–98 104–134.

Xu, X., Y. Che, Z. Yang, H. You, Y. Wang, and Y. Zhu (1992). Discussion of the seismogenic structure model for the Datong–Yanggao earthquake swarm, *Earthquake Res. China* **6**, no. 3, 361–371.

Department of Geology and Geophysics
University of Wisconsin-Madison
Madison, Wisconsin 53706
(T.L.M., H.F.W.)

Department of Earth Sciences
University of Hong Kong
Hong Kong
(L.S.C.)

Institute of Geology
State Seismological Bureau
Beijing 100029, China
(C.Y.)

Manuscript received 20 January 1999.